Applications of computational fluid dynamics to congenital heart diseases: a practical review for cardiovascular professionals

Taylor & Francis
Taylor & Francis Group

Expert Review of Cardiovascular Therapy

ISSN: (Print) (Online) Journal homepage: https://www.tandfonline.com/loi/ierk20

Applications of computational fluid dynamics to congenital heart diseases: a practical review for cardiovascular professionals

Gianluca Rigatelli, Claudio Chiastra, Giancarlo Pennati, Gabriele Dubini, Francesco Migliavacca & Marco Zuin

To cite this article: Gianluca Rigatelli, Claudio Chiastra, Giancarlo Pennati, Gabriele Dubini, Francesco Migliavacca & Marco Zuin (2021): Applications of computational fluid dynamics to congenital heart diseases: a practical review for cardiovascular professionals, Expert Review of Cardiovascular Therapy, DOI: 10.1080/14779072.2021.1999229

To link to this article: https://doi.org/10.1080/14779072.2021.1999229

Published online: 12 Nov 2021.

EXPERT REVIEW OF CARDIOVASCULAR THERAPY
https://doi.org/10.1080/14779072.2021.1999229

Taylor & Francis
Taylor & Francis Group

Applications of computational fluid dynamics to congenital heart diseases: a practical review for cardiovascular professionals

Gianluca Rigatelli[a], Claudio Chiastra [b], Giancarlo Pennati[c], Gabriele Dubini[c], Francesco Migliavacca [c] and Marco Zuin[d]

[a]Cardiovascular Diagnosis and Endoluminal Interventions Unit, Rovigo General Hospital, Rovigo, Italy; [b]PoliTo[BIO]Med Lab, Department of Mechanical and Aerospace Engineering, Politecnico di Torino, Turin, Italy; [c]Laboratory of Biological Structure Mechanics (Labs), Department of Chemistry, Materials and Chemical Engineering Giulio Natta, Politecnico di Milano, Milan, Italy; [d]Section of Internal and Cardiopulmonary Medicine, University of Ferrara, Ferrara, Italy

ABSTRACT

Introduction: The increased survival rate of patients with congenital heart disease (CHD) has made it likely that 70%–95% of infants with CHDs surviving into adulthood often require careful follow-up and (repeat) interventions. Patients with CHDs often have abnormal blood flow patterns, due to both primary cardiac defect and the consequent surgical or endovascular repair.

Area covered: Computational fluid dynamics (CFD) alone or coupled with advanced imaging tools can assess blood flow patterns of CHDs to both understand their pathophysiology and anticipate the results of surgical or interventional repair.

Expert opinion: CFD is a mathematical technique that quantifies and describes the characteristics of fluid flow using the laws of physics. Through dedicated software based on virtual reconstruction and simulation and patients' real data coming from computed tomography, magnetic resonance imaging, and 3/4 D-ultrasound, reconstruction of models of circulation of most CHD can be accomplished. CFD can provide insights about the pathophysiology of coronary artery anomalies, interatrial shunts, coarctation of the aorta and aortic bicuspid valve, tetralogy of Fallot and univentricular heart, with the capability in some cases of simulating different types of surgical or interventional repair and tailoring the treatment on the basis of these findings.

ARTICLE HISTORY
Received 2 February 2021
Accepted 25 October 2021

KEYWORDS
Congenital heart disease; computer simulations; computational fluid dynamics; pathophysiology; therapy

1. Introduction

Congenital heart disease (CHD) has an incidence of 8 per 1000 births [1]. Advances in diagnostics, perioperative care, surgical and in particular endovascular techniques increased the survival rate of patients with CHD but unfortunately, although 70%–95% of infants with CHDs survive into adulthood [2], the rate of long-term morbidity, which often requires (repeat) intervention, has increased over the last decades. Patients with CHDs have often abnormal blood flow patterns, due to both primary cardiac defect and the consequent surgical or endovascular repair [3].

These abnormal blood flow patterns may contribute to impairing cardiac and vascular functions increasing the likelihood of recurrent hospitalizations and repeated interventions. In this regard, since the pioneering work of de Leval and colleagues in 1996 [4], computational fluid dynamic (CFD) is increasingly offering a unique chance to understand pathophysiology of CHDs before and after intervention and to tailor the proper repair to the specific patients before the intervention [5].

The aim of the present review is to outline the findings of CFD in the study of pathophysiology of different CHDs and its applications to endovascular and surgical repair planning.

2. Computational fluid dynamics

2.1. Definition

CFD is a technique based on computer simulations used to analyze systems involving fluid flow [6]. CFD is suitable for a wide range of industrial and non-industrial application areas, including aircraft and automotive aerodynamics, ship hydrodynamics, turbomachinery, meteorology, and biomedical engineering, among the others [7]. In cardiovascular field, CFD is usually used to investigate the blood flow patterns within the heart and/or the vessels by considering the laws of physics that describe the fluid motion. The biological effects, such as auto-regulation, healing, and growth, and so on, are seldom modeled. More in detail, the governing equations of fluid motion are the continuity equation (eq. 1), deriving from the mass conservation, and the Navier-Stokes equations (eq. 2), deriving from the momentum conservation, which can be expressed in case of incompressible and Newtonian fluid as follows

$$\cdot v = 0 \quad (1)$$

CONTACT Gianluca Rigatelli jackyheart@libero.it Cardiovascular Diagnosis and Endoluminal Interventions, Santa Maria Della Misericordia Hospital, Viale Tre Martiri 140, Rovigo 45100, Italy

Article highlights

- Patients affected by congenital heart disease are increasingly reaching the adulthood, usually having abnormalities of the cardiac blood flow patterns due to the cardiac abnormalities or/and the related surgery
- Assessment of the blood flow patterns can be very difficult, in particular in operated patients with current imaging tools
- Computational fluid dynamics alone or coupled with current imaging techniques can be used to understand the underlying pathophysiology of congenital heart disease
- Computational fluid dynamics alone or coupled with current imaging techniques can be used to model different types of surgical and interventional procedures, anticipating their results and helping in planning patient-tailored procedures

$$\rho\left[\frac{\partial v}{\partial t} + v \cdot \quad v\right] = - \quad p + \mu \quad ^2 v + \rho g \tag{2}$$

where ∇ is the gradient operator, $\boldsymbol{v}$ the velocity vector, ρ is the blood density, t is the time, p is the pressure, $\boldsymbol{g}$ is the gravity. These non-linear, partial differential equations cannot be solved analytically in case of complex three-dimensional geometries. Thus, numerical techniques, usually based on the finite volume or finite element method, are adopted to solve the discretized form of the equations within CFD software packages [7]. First, by means of the volume meshing, the fluid domain (i.e. continuum of interest) is subdivided into smaller, non-overlapping sub-domains called elements. Secondly, the governing equations are integrated over all the elements of the domain and then converted into a system of non-linear algebraic equations. Lastly, the resulting set of algebraic equations (often in the order of millions of equations) is solved using computer workstations or high-performance computing clusters. Nowadays, the current capability of parallel computer processing allows the solution of the governing equations of fluid motion under non-steady condition in complex anatomies within reasonable computational time. Typically, resolving a time-accurate model can require one or more days of computations, considering a fluid domain discretized into one million elements (or more) and few cardiac cycles, each subdivided into hundreds of timesteps [8].

2.2. CFD analysis: workflow

The main steps of a patient-specific CFD analysis are summarized in Figure 1 [9,10]. Vessels and cardiac chambers are virtually reconstructed based on the measurements of vessel size and length obtained by quantitative coronary angiography, computed tomography or MRI analyses or, in the field of coronary artery anomalies, by processing intravascular images (i.e. intravascular ultrasound or optical coherence tomography). Typically, the computational grid is characterized by tetrahedral (or hexahedral) elements within the fluid domain and a boundary layer close to the wall, which is introduced to better capture the high-velocity gradients at the wall. Thirdly, the set-up of the CFD simulation is defined. In particular, the physical model (e.g. unsteady flow with or without the inclusion of a turbulent model), blood properties (i.e. blood density and viscosity), initial conditions, boundary conditions, and solver settings are set. The definition of the initial conditions and boundary conditions, which are prescribed values of the calculated quantities (i.e. velocity and pressure) at certain times and locations, is needed for the resolution of the governing equations.

To extract the boundary conditions from different imaging techniques makes the CFD simulations patients' specific and more realistic [11,12]: consequently, in order to formulate a well-posed problem, most researchers must guess parameters such as flow boundary conditions, vessel wall properties, and sometimes even geometric vessel parameters if patient imaging is not of sufficient quality. It has been shown that these factors and others can significantly alter the flow solution. It is critical to determine the amount of uncertainty introduced by the flow's inlet and outlet conditions, since they are difficult and expensive to measure, in order to evaluate the degree to which cardiovascular flow simulations are accurate. As a matter of fact the outlet boundary conditions influence a larger percent of the solution domain. Boundary conditions can be derived from imaging data or experimental measurements, such as MRI data, Doppler ultrasound, catheter-based pressure and velocity measurements or transesophageal echocardiography: more accurate they are, more realistic becomes the simulation. Fourth, the CFD simulation is run on a computer

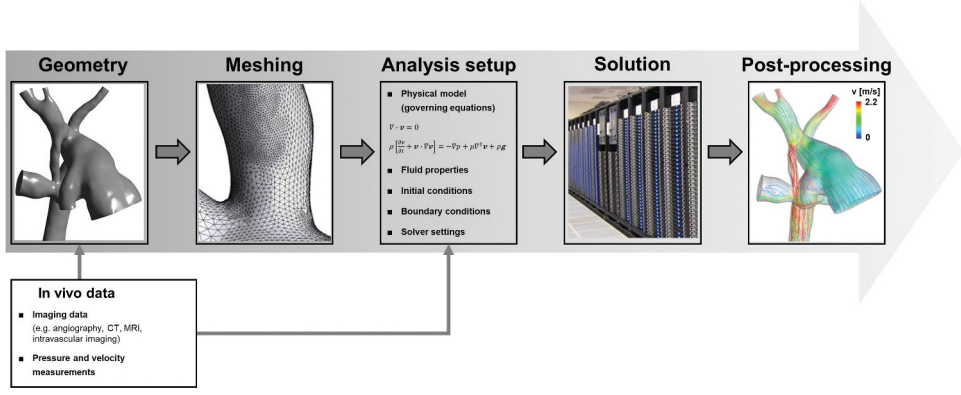

Figure 1. Main steps of patient-specific CFD analyses in the field of CHD. Images inspired from Corsini C et al [51].

Table 1. Examples of flow phenomena that can be characterized by CFD with the calculation of specific hemodynamic quantities.

Flow phenomena	Hemodynamic quantities
Pressure field	Static pressure, dynamic pressure, total pressure, pressure drop
Flow distributions Flow energy losses	Energetic performance indexes derived from the velocity vector field
Abnormal flow patterns (including re-circulating flows, stagnation flow, vortexes)	Velocity, vorticity
Distribution of wall shear stress along the wall surface	Wall shear stress – based descriptors (e.g. time-averaged wall shear stress, oscillatory shear index, wall shear stress gradient, etc.)

workstation or high-performance computing cluster by taking advantage of their parallel computing features. Lastly, the solution of the CFD analysis is obtained and the results are post-processed in order to extract the hemodynamic quantities of interest, detailed in the following sub-section.

Virtual endovascular or surgical interventions can be simulated after 3D computer reconstruction of the stent, valve or conduit, adding material properties, elasticity, rigidity, diameter, length and put into the software all the steps of the simulated procedure (for example, atmosphere of balloon inflation, duration of the inflation, postdilatation, etc.). Then the results of such interventions can be evaluated by 0-dimensional and 1 dimensional models. Zero-D models provide a concise way to evaluate the hemodynamic interactions among the cardiovascular organs, whilst one-D (distributed parameter) models add the facility to represent efficiently the effects of pulse wave transmission in the arterial network at greatly reduced computational expense compared to higher dimensional computational fluid dynamics studies [13].

2.3. CFD analysis: quantities of interest

The main flow phenomena in this field that can be characterized by CFD and the corresponding hemodynamic quantities of interest are reported in Table 1. The hemodynamic parameters derived from both pressure and velocity fields are analyzed. The pressure in the vessels and chambers is expressed in pascal (Pa) or mmHg, according to the International System of Units. The vorticity magnitude (expressed in 1/s) is defined as the magnitude of the vorticity vector; the vorticity vector is a measure of the rotation of a fluid element as it moves through the domain and it may be representative of pathological conditions when far from the baseline [14]. The wall shear stress (WSS) (expressed in Pa), is defined as the frictional force of the flowing blood along the wall surface per unit area. WSS values deflecting from a baseline value are indexes of abnormalities leading to thrombus formation, abnormal vessel modeling and pathological remodeling, arterial damage [15]. Another important quantity to be evaluated is the power (energy per unit time, measured in watt) dissipated when the blood flows in arteries. Minimizing this loss of energy when designing or re-routing the blood in surgical connections is an index of a good streamlining of the blood [4].

3. Embryonicheart development

Hemodynamic begins shaping the growth of the developing heart from the early embryonic stages. Blood circulation starts with the beating of the primitive tubular heart (around the beginning of the fourth gestational week in human development) [16]. From this time on, the dynamics of blood flow regulates many aspects of cardiovascular development. For instance, genesis of vessels and capillaries, and even differences between arterial and venous phenotypes, are determined by blood flow characteristics [9]. In the heart, the interaction between blood flow and cardiac tissues also determines how the heart continues to develop [17,18]. The understanding of these types of blood flow help identify the causes of congenital heart malformation. Detailed CFD models of both the developing vasculature and the heart, together with experimental data on adaptations to blood flow, have been undertaken in zebrafish and chick's embryo heart in order to elucidate important aspects of the complex mechanisms by which blood flow dynamics regulates cardiovascular growth and development. In humans the models so far are based on four-dimensional ultrasound scans of 20-week-old normal human fetuses. Image analyses of ultrasound scans revealed the motion of the heart walls that was used in the generation of CFD models of the fetuses' left and right ventricles. In both left and right ventricles, CFD simulations of fetal heart, imaged by echocardiogram, reveal complex flow patterns and the presence of flow vortex rings, which generate significant WSS on the endocardium, potentially playing an important role on cardiac efficiency [19]. Indeed, CFD enables the quantification of WSS, which is otherwise extremely difficult using only in vivo measured flow data. Detailed CFD models of both the developing vasculature and the heart, together with experimental data on adaptations to blood flow, are starting to elucidate important aspects of the intricate mechanisms by which blood flow dynamics regulates cardiovascular growth and development. Wall shear stresses play a substantial role in cardiovascular adaptations to flow, but they are difficult to estimate using only measured flow data. Once blood flow dynamics have

been simulated, CFD models offer the advantage of relatively easy quantification of wall shear stresses on endothelial and endocardial walls, derived from flow variables.

4. CFD applications to congenital heart disease

Table 2. Congenital heart diseases evaluable by CFD and inherent purposes.

Disease	Pathophysiology	Intervention simulation/ planning
Coronary artery anomalies	+++	+++
Atrial septal defect/Patent foramen ovale	++	±
Coarctation of aorta	+++	+++
Bicuspid aortic valve	+++	+
Tetralogy of Fallot	++	+
Pulmonary valve insufficiency	+	+++
Norwood circulation	+++	++
Fontan circulation	+++	+++

+++: very useful; ++ moderately useful; + poorly useful; – non useful

CFD has been applied in the past and is currently used in different CHDs in order to both understand pathophysiology, and anticipate and plan surgical or interventional procedures (Table 2).

4.1. Congenital coronary artery anomalies

Coronary artery anomalies (CAAs) occur in 0.64% to 5.60% of patients undergoing coronary angiography [20,21]. The majority of CAAs pathophysiology and clinical history have been fully clarified in the past 30 years. Myocardial bridges and anomalous origin from the opposite sinus (ACAOS) constitute the most clinically investigated pathologies among the wide spectrum of coronary artery anomalies (CAAs), since they have been related with myocardial infarction and sudden cardiac death [22].

Myocardial bridges (MB) were assessed by Javadzadegan et al. [23] using CFD, by dividing patient-specific myocardial bridge models (n = 10) by length. A direct relationship between myocardial bridge length and hemodynamic perturbations emerged in this study. Long myocardial bridge length seems to be associated with lower WSS and higher residence time in the proximal segment to the bridge, and a higher WSS and shorter residence time within the bridge, as compared to short length. More recently Sharzehee M et al. [24] showed that increasing the MB length (by 140%) only had significant impact on the pressure drop in the severe MB (39% increase at the exercise). However, increasing the stenosis length dramatically increased the pressure drop in both moderate and severe stenoses at all flow rates (31% and 93% increase at the exercise, respectively). Both CFD and experimental results confirmed that the MB had a higher maximum and a lower mean pressure drop in comparison with the stenosis, regardless of MB/stenosis severity.

The description of ACAOS is currently based on the terminology introduced by Angelini et al. [25], which includes an L or R prefix to indicate the (Right or Left) coronary artery involved and a suffix to indicate the proximal course: intramural (IM), pre-pulmonic (PP), subpulmonic (SP), retro-aortic (RA), retrocardiac (RC) and wrapped around the apex (WA). Rigatelli et al. computationally investigated the pathophysiology of Left ACAOS with and without IM course [26]. After reviewing both the angiographic and computed tomography findings of 13 consecutive athletes, CFD models were created to simulate the conditions of extreme effort. In particular, vorticity magnitude, static pressure, and WSS were analyzed in models of L-ACAOS with no IM course and L-ACAOS-IM at rest and during exercise. The mean vorticity magnitude and WSS significantly increased from rest to exercise in both models, in the right coronary artery, left anterior descending, and left circumflex coronary arteries. The mean static pressure (1.118e+004 vs 1.164e+004 Pa, $p < 0.001$), as well as the mean vorticity magnitude and mean WSS (7012.78 1/s vs 9019.56 1/s, $p < 0.001$, $\Delta = 2006.78$ 1/s and 3.02 Pa vs 2.11 Pa, $p < 0.001$, $\Delta = 0.91$ Pa) significantly increased with exercise in the L-ACAOS-IM model. This net increment was transmitted to the entire left coronary system in L-ACAOS-IM but not in L-ACAOS with no IM. More recently, we analyzed the pathophysiology of L- and R-ACAOS with IM course in relation to eventual stenting of the IM course [27] suggesting that the phasic stenosis inside IM ('squeezing') can be produced by a combined mechanism of compression and twisting, which causes a net pressure reduction drop leading to myocardial ischemia (Figure 1). These hypotheses seem in part confirmed by the study of Razavi et al. [28] which showed that different flow patterns exist natively between right and left anomalous coronary arteries. Surgical unroofing of the vessel may normalize time-averaged WSS but with variance related to the AO.

CFD in this context helped to define the mechanism of myocardial ischemia in ACAOS which seems to be induced by compression and squeezing of the intramural segment (IM) with pressure drop at its end.

4.2. Interatrial shunts

Interatrial shunts include patent foramen ovale (PFO), secundum atrial septal defect (secundum ASD), sinus venosus ASD and ostium primum ASD [29]. There are very few studies about CFD in interatrial shunts. Rigatelli et al. investigated the pathophysiology of right-to-left shunting in patients with patent foramen ovale by means of CFD [30]. In this study, the right

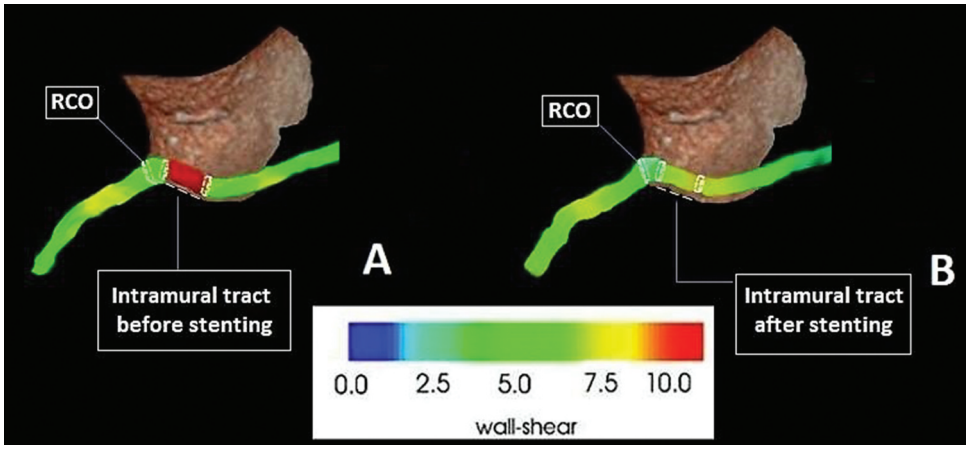

Figure 2. Computational fluid dynamics simulation of a right anomalous coronary origin from the opposite sinus with particular focus on the intramural course before (A) and after (B) stenting. Note the changing in the wall shear stress within the intramural segment and along the coronary artery.

and left atrial chambers connection from MRI data of a pool of patients with mild or permanent right-to-left (RL) shunting was reconstructed. By performing CFD simulations, a higher vorticity was observed in the case of permanent R-L shunt involving the wall of the left atrium (LA), especially at the left atrial appendage (LAA, Figure 2). Conversely, when the degree of the shunt diminished, the vorticity in the same area resulted lower. Moreover, a marked gradient of total pressure (defined as the sum of static and dynamic pressures, measured in pascal (Pa) was found across the PFO. A higher vorticity magnitude was observed in the permanent shunt both in the LA (117.32 vs 110.25, p = 0.001) and at the LAA (33.29 vs 21.25, p = 0.001) when compared to mild shunt. CFD confirmed a potential additional mechanism of PFO-mediated embolism: the stagnation of blood flow in LA in patients with permanent RL shunt suggested by the high vortex magnitude potentially increases chance of microthrombi formation in the LA: this hypothesis has been clinically postulated years ago [31] and finally found a confirmation by CFD.figure 3

Rigatelli et al. demonstrated that such an abnormal flow pattern assessed by CFD can be worsened in terms of aberrant distribution of aortic WSS by a concomitant coronary artery disease of proximal major coronary arteries such as the left main stem [36]. Some authors comparing the blood flow in BAV versus normal (non-dilated) aortas with tricuspid aortic valves by means of CFD analyses showed an altered WSS distribution in all different BAV fusion types [37,38]. Both 4D-flow cardiovascular MRI and CFD analyses showed abnormal WSS distribution in patients with BAV even before aortic dilation occurs, suggesting that abnormal WSS could precede anatomical remodeling of the aorta. WSS monitoring in addition to routine aortic dimensions has the potential to allow early identification of young asymptomatic patients at risk of progression of aortopathy [39], guiding the surgeon to reinforce the aortic sites at increased risk, as recently suggested [40].

4.3. Bicuspid aortic valve

Bicuspid aortic valve (BAV), which is not only associated with valve dysfunction but also with aortic pathology such as aortic dilatation and even dissection, represents the most common congenital heart abnormality [32]. The abnormal arrangement of the aortic valve leaflets in BAV generates an abnormal flow pattern in the ascending aorta depending on the type of leaflet fusion [33,34]. Emendi et al. [35] demonstrated that fluid-structure interaction derived from RMI predicted direction and magnitude of the flow jet impinging onto the aortic

4.4. Coarctation of the aorta

Coarctation of the aorta (CoA) is a narrowing of the upper descending thoracic aorta, generally distal to the origin of the left subclavian artery near the insertion of the ligamentum arteriosum. CoA accounts for approximately 5%–8% of all CHDs [41]. The diagnostic imaging tools currently used in clinical practice provide dimensions, velocities, and pressure gradients, but cannot characterize the aortic blood flow and its effects on the aortic wall. CFD coupled with cardiac MRI can offer a more comprehensive evaluation of the transaortic

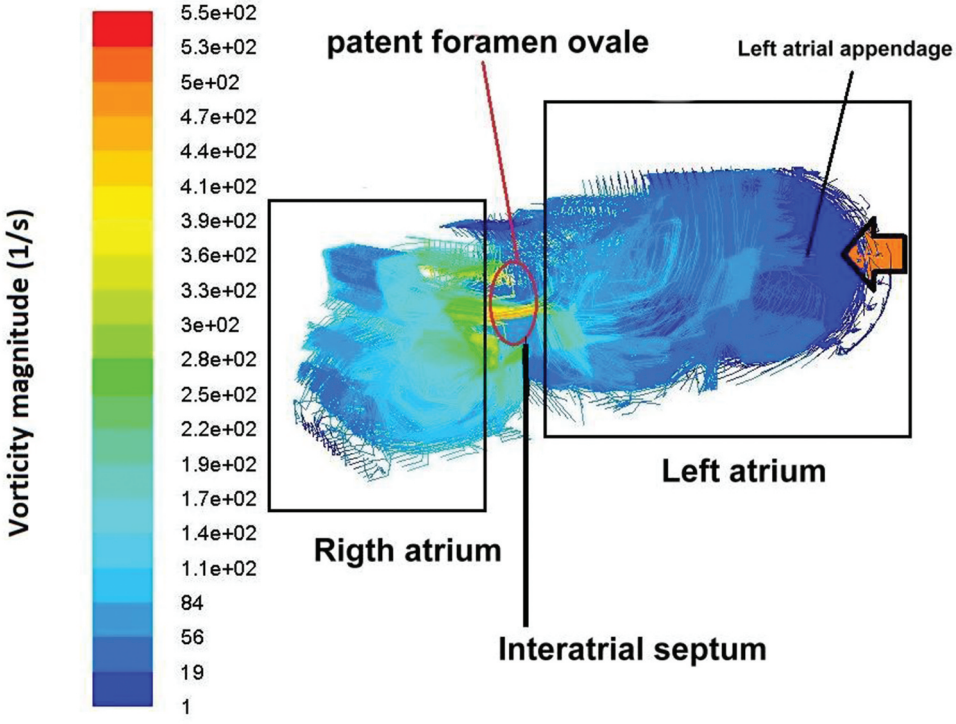

Figure 3. Computational fluid dynamics investigation of a patient with a high-grade Right-to-Left shunt (permanent shunt without Valsalva) through a patent foramen ovale, demonstrating a region of stagnant flow (blue), usually not present in patients with no or mild shunt.

gradient, which is usually uncorrected in sedated patients, and blood flow patterns inside the aorta and anticipating the potential effects of stenting or surgical repair [42]. CFD has been used for surgical planning in patients to aid surgeons and physicians in clinical decision making [43,44]. Models of the patient's anatomy after several different types of surgery or stenting can be generated, and CFD analyses based on patient-specific boundary conditions can be performed to assess the expected hemodynamic after surgery. Capelli et al. [45] used CFD tools to identify the maximum expansion diameter of the aorta allowed for the covered stent at the level of the narrowing in the descending aorta in order to avoid obstruction of the origin of the aberrant right subclavian artery and compression of the bronchi. The CFD analyses quantified a decrease in the peak velocity as well as the pressure gradient, which in all the virtually treated CoA dropped from an average of 15.5 mmHg pre-implant to 1.9 mmHg after stenting, anticipating the results obtained in the real patients in the cath-lab (Figure 4).

CFD in aortic coarctation has the potential to anticipate the decrease in pressure gradient after stenting and to select the proper stent length.

4.5. Tetralogy of Fallot

The Tetralogy of Fallot (ToF) is a major congenital cardiac disease including pulmonary stenosis, ventricular septal defect, overriding aorta and right ventricle (RV) hypertrophy, which result in cyanosis and accounts for 7%–10% of all CHDs [46]. The surgical widening of the right ventricular outflow tract usually produces a certain degree of pulmonary valve regurgitation (PR), which can result in RV volume and pressure overload over time. PR could also play a role in the formation of vortex flow in PAs, although the etiology is still poorly understood. In general, flow vortices are associated with alteration in WSS and affect endothelial function [47]. CFD could potentially identify parameters suitable for the prediction of outcomes in patients with repaired ToF and refine the timing for pulmonary valve replacement. Moreover, CFD coupled with virtual procedure simulation could be used to anticipate the results and tailor possible percutaneous pulmonary valve implantation according to the patients' anatomy and flow patterns, as already showed by Capelli et al. [48].

4.6. Univentricular heart

Patients with only a single functional ventricle usually undergo consecutive palliative surgery resulting in a three-stage procedure [48,49]: a) Norwood procedure [Blalock–Taussig shunts, central shunts, right ventricle-to-pulmonary artery conduit and the hybrid Norwood], (b) Glenn or hemi-Fontan procedures, and (c) complete Fontan procedure (or total cavopulmonary connection) in which the superior and inferior caval veins are connected to the PA. The completion of the Fontan circulation can be done with either the extra cardiac conduit or the lateral tunnel approach [50].

4.7. Norwood circulation

Migliavacca et al. [51] investigated the Norwood circulation by means of CFD analyzing the shunt pressure drop–flow relationships, varying shunt implantation angles, diameter, curvature, and input pulsatility and found, as expected, that shunt diameter was the main determinant of graft flow. The researchers found that most of the pressure drop occurred close to the proximal anastomosis, and curved grafts resulted in a lower pressure drop as compared with straight grafts, due to reduced flow-line skewness toward the lateral graft wall near the proximal anastomosis. Subsequently, the same research group compared the variants of the Norwood reconstructive surgeries

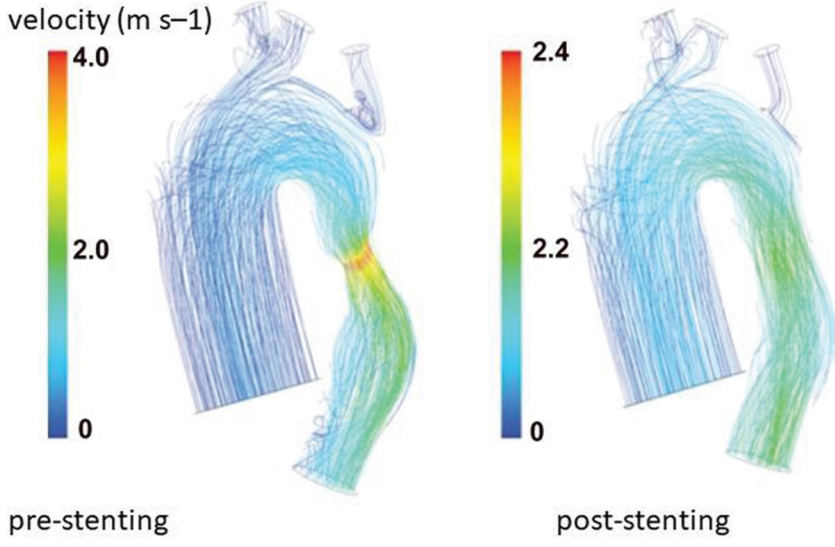

Figure 4. Comparison of the velocity streamlines for an aortic coarctation (CoA) before and after the virtual implantation of a stent to relieve the restriction of the descending aorta. Within the post-stenting geometry, the peak velocity decreases and the downstream flow is less disturbed (with permission from Capelli et al [42]).

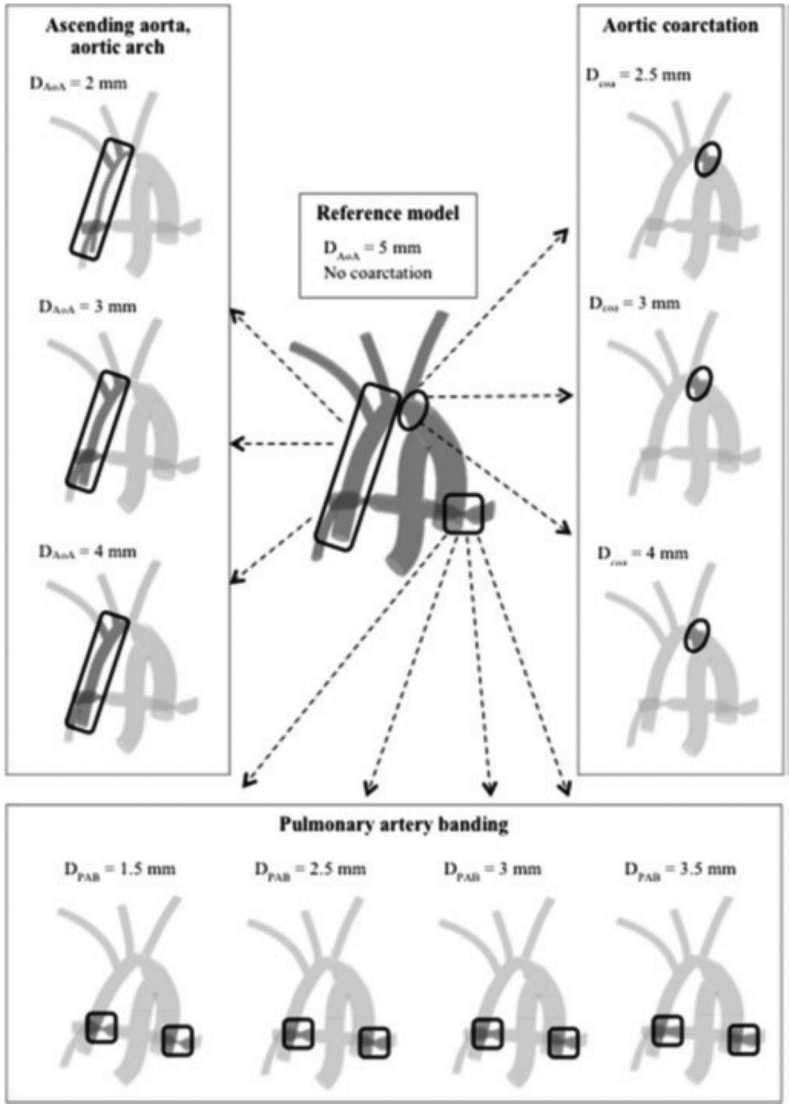

Figure 5. **T**Hree-dimensional models of the hybrid Norwood operation with varying ascending aorta and aortic arch diameters (left, DAoA), aortic coarctation diameters (right, Dcoa), and PA banding diameters (bottom, DPAB). The model considered as a reference is depicted in the center. On these models CFD can be applied to understand changes of blood flow throughout the different morphologies (modified from Baker et al [50]).

with post-operative catheterization and Doppler data by carrying out a multi-scale CFD analysis [52]. The Norwood operation with a modified Blalock–Taussig shunt was compared with the right ventricle to pulmonary artery shunt modification. The model predicted that the right ventricle shunt would result in higher aortic diastolic pressure, decreased pulmonary arterial pressure, lower pulmonary to systemic flow, and higher coronary perfusion relative to the innominate artery-to-right pulmonary artery shunt. CFD by means of simulation of different diameter and length of shunt can be used to predict which configuration allows for the most favorable hemodynamic pattern [53] (Figure 5).

4.8. B) Fontan circulation

The hemodynamic assessment in Fontan circulation is difficult because of the abnormal position and geometry of the systemic ventricle, the extent of the Fontan circuit and the passive nature of flow to the pulmonary circulation. Blood flow to the pulmonary circulation in Fontan patients is subjected to the intrathoracic pressure changes during respiration, systemic venous pressure, systolic and diastolic performance of the systemic ventricle, and the peripheral muscle pump. As already suggested [54], energy loss within the total caval-pulmonary connection is an important factor for Fontan hemodynamic and should be minimized as much as possible acting on vessel size, anastomosis shape, total blood flow, and pulmonary/caval flow distribution [55,56].

Haggerty et al. [57] used CMR-based CFD to evaluate the hemodynamic profiles in 100 Fontan patients, with a focus on power loss within the Fontan circuit, showing that stenosis in the Fontan tunnel and undersized pulmonary arteries were associated with increased power loss, thereby having a clearly negative effect on Fontan hemodynamic. Rijnberg FM recently using CFD that hepatic venous flow is non-uniformly distributed within the Fontan conduit and that individual

inaccuracies in hepatic fluid distribution quantification potentially having a clinical impact [58].

CFD was used for surgical planning in such patients to aid surgeons and physicians in clinical decision making [59] providing insight into preoperative blood flow. Models of the patient's anatomy after several different types of surgery can be virtually generated, and patient-specific boundary conditions can be used to assess the expected hemodynamic after surgery [60,61]. On this regard, Tang et al. [62] suggested recently the use of a rigid wall assumption on evaluation of time-averaged intra-atrial total cavopulmonary connection hemodynamic metric under resting breath-held condition.

5. Conclusions

CFD alone as virtual simulation of real phenomena in CHD, or coupled with MRI and 3D ultrasound data, offers a unique opportunity to understand not only the cardiac development and potential congenital abnormalities, but also the pathophysiology of CHDs. Furthermore, in several cases, CFD can help anticipate the results of surgical or interventional repair in terms of flow patterns and WSS.

6. Expert opinion

CFD has been applied to CHDs since the early 1990s in order to investigate pathophysiology of complications from extensive surgical repair such as the Norwood or Fontan operations. The basis of CFD and related simulations have remained substantially the same since their postulation in the '80s and '90s. With the development of more efficient and robust software three-dimensional vessel reconstruction and execution of hemodynamic analysis, the field of application of CFD has recently moved to the assessment of more common CHDs such as interatrial shunts and coarctation [63]. The availability and demonstrated efficacy of the transcatheter valvular implantation [64] at both tricuspid and pulmonary sites in order to repair the well-known complication of Tetralogy of Fallot has induced a rise in the application of CFD is such a field aimed to select a patient's specific device (Figure 6) or to predict complication of valve implantation (e.g. frame fracture). Clearly, some points of improvement do exist. First, a more open knowledge is needed of geometrical characteristics and mechanical properties of the current devices – atrial septal defect occlusion devices, coarctation stents, and transcatheter valves – which are hardly widely available and would be essential for building up realistic computational models to perform CFD analyses. Secondly, use of established models of different CHDs already available for clinical application as in the percutaneous coronary field has begun to happen. Thirdly, the development of validated three-dimensional vessel reconstruction and CFD software, easily accessible within the hospital to operators without biomechanical engineering background, including clinicians and radiologist technicians. Lastly, the decrease in price of the specific software should be advocated in order to expand the adoption of such a technology all-over the world, in particular in less developed areas where paradoxically CHDs tend to be more and more prevalent.

Further improvement in the quality of available virtual simulation software and the enhanced capabilities of coupling with existing in vivo diagnostic tool as MRI, 3D and 4D ultrasound, optical coherence tomography, intravascular ultrasound imaging, and angiographic equipment are likely to push forward such a technology in the clinical practice making the transition from off-line assessment and planning to on-line evaluation and treatment more effective.

Acknowledgments

We thank Prof Aravinda Nanjundappa, Robert C. Byrd Clinical Training Center, Vascular Center of Excellence, West Virginia University, Charleston, WV, for the English language editing.

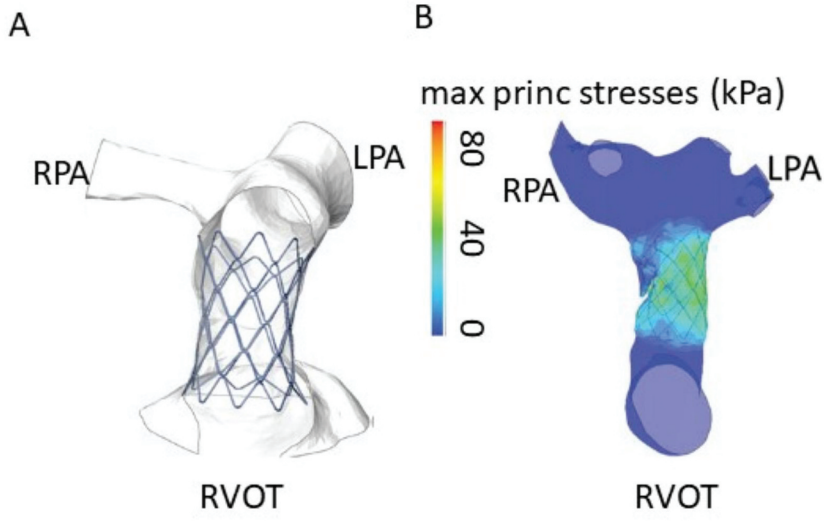

Figure 6. **S**imulations of feasible pulmonary percutaneous valve implantation: (a) deformed configuration of Melody stent virtually implanted (frontal view cut); and (b) stress distribution following the stent implantation (modified from Capelli et al [42]).

Funding

This paper was not funded.

Declaration of interest

The authors have no relevant affiliations or financial involvement with any organization or entity with a financial interest or financial conflict with the subject matter or materials discussed in the manuscript. This includes employment, consultancies, honoraria, stock ownership or options, expert testimony, grants or patents received or pending, or royalties.

Reviewer disclosures

Peer reviewers on this manuscript have no relevant financial or other relationships to disclose.

ORCID

Claudio Chiastra http://orcid.org/0000-0003-2070-6142
Francesco Migliavacca http://orcid.org/0000-0003-4644-630X

References

Papers of special note have been highlighted as either of interest (•) or of considerable interest (••) to readers.

1. Hoffman JIE, Kaplan S. The incidence of congenital heart disease. J Am Coll Cardiol. 2002;39:1890–1900.
2. Oster ME, Lee KA, Honein MA, et al. Temporal trends in survival among infants with critical congenital heart defects. Pediatrics. 2013;131:e1502–8.
3. Bove EL, de Leval MR, Migliavacca F, et al. Computational fluid dynamics in the evaluation of hemodynamic performance of cavopulmonary connections after the Norwood procedure for hypoplastic left heart syndrome. J Thorac Cardiovasc Surg. 2003;126:1040–1047.
4. de Leval MR, Dubini G, Migliavacca F, et al. Use of computational fluid dynamics in the design of surgical procedures: application to the study of competitive flows in cavo-pulmonary connections. J Thorac Cardiovasc Surg. 1996 Mar; 111(3):502–513.**••First CFD study in literature**
5. Gerrah R, Haller SJ. Computational fluid dynamics: a primer for congenital heart disease clinicians. Asian Cardiovasc Thorac Ann. 2020 Oct;288:520–532. Epub 2020 Sep 2. PMID: 32878458.
6. Theodorakakos A, Gavaises M, Andriotis A, et al. Simulation of cardiac motion on non-Newtonian, pulsating flow development in the human left anterior descending coronary artery. Phys Med Biol. 2008;53:4875–4879.
7. Cho Y, Kensey KR. Effects of the non-Newtonian viscosity of blood on flows in a diseased arterial vessel. Part 1: steady flows. Biorheology. 1991;8:241–262.**••pivotal article giving the theoretical basis for CFD analysis.**
8. Morris PD, Narracott A, Von Tengg-kobligk H, et al. Computational fluid dynamics modelling in cardiovascular medicine. Heart. 2016 Jan;102(1):18–28.
9. Pennati G, Corsini C, Hsia TY, et al. Modeling of Congenital Hearts Alliance (MOCHA) Investigators. Computational fluid dynamics models and congenital heart diseases. Front Pediatr. 2013 Feb 26;1:4. PMID: 24432298; PMCID: PMC3882907.**•important article of CFD application in CHDs.**
10. Arbia G, Esmaily Moghadam M, Marsden AL, et al. Modeling of Congenital Hearts Alliance (MOCHA) Investigators. Numerical blood flow simulation in surgical corrections: what do we need for an accurate analysis? J Surg Res. 2014 Jan;1861:44–55. Epub. 2013 Aug 11.
11. Madhavan S, Kemmerling EMC. The effect of inlet and outlet boundary conditions in image-based CFD modeling of aortic flow. Biomed Eng. 2018 May 30;17(1):66. Online. PMID: 29843730; PMCID: PMC5975715.
12. Pirola S, Cheng Z, Jarral OA, et al. On the choice of outlet boundary conditions for patient-specific analysis of aortic flow using computational fluid dynamics. J Biomech. 2017 Jul 26;60:15–21. Epub. 2017 Jun 20. PMID: 28673664.
13. Shi Y, Lawford P, Hose R. Review of Zero-D and 1-D models of blood flow in the cardiovascular system. BioMed Eng. 2011;10:33. OnLine.
14. Jamalidinan F, Hassanabad AF, François CJ, et al. Four-dimensional-flow magnetic resonance imaging of the aortic valve and thoracic aorta. Radiol Clin North Am. 2020 Jul;58(4):753–763.
15. Morbiducci U, Kok AM, Kwak BR, et al. Atherosclerosis at arterial bifurcations: evidence for the role of haemodynamics and geometry. ThrombHaemost. 2016 Mar;115(3):484–492.
16. Lindsey SE, Butcher JT, Yalcin HC. Mechanical regulation of cardiac development. Front Physiol. 2014;5:318.
17. Sato Y, Poynter G, Huss D, et al. Dynamic analysis of vascular morphogenesis using transgenic quail embryos. PLoS ONE. 2010;5:e12674.
18. Hierck BP, Van der Heiden K, Poelma C, et al. Fluid shear stress and inner curvature remodeling of the embryonic heart. Choosing the right lane! Sci World J. 2008;8:212–222.
19. Courchaine K, Rugonyi S. Quantifying blood flow dynamics during cardiac development: demystifying computational methods. Philos Trans Royal Soc B. 2018;373:20170330.
20. Kardos A, Babai L, Rudas L, et al. Epidemiology of congenital coronary anomalies: a coronary arteriography study on a central European population. Cathet Cardiovasc Diagn. 1997;42:270–275.
21. Yamanaka O, Hobbs RE. Coronary artery anomalies in 126,595 patients undergoing coronary arteriography. Cathet Cardiovasc Diagn. 1990;21:28–40.
22. Rigatelli G, Rigatelli A, Cominato S, et al. A clinical-angiographic risk scoring system for coronary artery anomalies. Asian Cardiovasc Thorac Ann. 2012;20:299–303.
23. Javadzadegan A, Moshfegh A, Fulker D, et al. Development of a computational fluid dynamics model for myocardial bridging. J Biomech Eng. 2018;140. DOI:10.1115/1.4040127. in press.
24. Sharzehee M, Seddighi Y, Sprague EA, et al. A hemodynamic comparison of myocardial bridging and coronary atherosclerotic stenosis: a computational model with experimental evaluation. J Biomech Eng. 2020 Dec 3; doi:10.1115/1.4049221. Epub ahead of print. PMID: 33269788.
25. Angelini P, Uribe C. Anatomic spectrum of left coronary artery anomalies and associated mechanisms of coronaryinsufficiency. Catheter Cardiovasc Interv. 2018;92:313–321. in press.**•important article about the pathophysiology and clinical impact of congenital coronary anomalies.**
26. Rigatelli G, Zuin M, Galasso P, et al. Mechanisms of Myocardial Ischemia Inducing Sudden Cardiac Death in Athletes with Anomalous Coronary Origin from the Opposite Sinus: insights from a computational fluid dynamic study. Cardiovasc Revasc Med. 2019 Dec;20(12):1112–1116.
27. Rigatelli G, and Zuin M. Computed tomography-based patient-specific biomechanical and fluid dynamic study of anomalous coronary arteries with origin from the opposite sinus and intramural course. Heart Int. 2020;14(2):105-111. doi:10.17925/HI.2020.14.2.105.
28. Razavi A, Sachdeva S, Frommelt PC, et al. Patient-specific numerical analysis of coronary flow in children with intramural anomalous aortic origin of coronary arteries. Semin Thorac Cardiovasc Surg. 2020 Aug 26;S1043-0679(20)30271–9. doi:10.1053/j.semtcvs.2020.08.016. Epub ahead of print. PMID: 32858220.
29. Rigatelli G, Zuin M, Nghia NT. Interatrial shunts: technical approaches to percutaneous closure. Expert Rev Med Devices. 2018;15(10):707–716.
30. Rigatelli G, Zuin M, Fong A. Computational flow dynamic analysis of right and left atria in patent foramen ovale: potential links with atrial fibrillation. J Atr Fibrillation. 2018;10(5):1852.

31. Yener N, Oktar GL, Erer D, et al. Bicuspid aortic valve. Ann Thorac Cardiovasc Surg. 2002;8:264–267.
32. Piatti F, Sturla F, Bissell MM, et al. 4D flow analysis of BAV-related fluid-dynamic alterations: evidences of wall shear stress alterations in absence of clinically-relevant aortic anatomical remodelling. Front Physiol. 2017;8:441.
33. Meierhofer C, Schneider EP, Lyko C, et al. Wall shear stress and flow patterns in the ascending aorta in patients with bicuspid aortic valves differ significantly from tricuspid aortic valves: a prospective study. Eur Heart J Cardiovasc Imaging. 2013;14:797–804.
34. Emendi M, Sturla F, Ghosh RP, et al. Patient-specific bicuspid aortic valve biomechanics: a magnetic resonance imaging integrated fluid-structure interaction approach. Ann Biomed Eng. 2020 Aug 17; doi:10.1007/s10439-020-02571-4. Online ahead of print. PMID: 32804291.
35. Rigatelli G, and Zuin M. Left main stenosis stenting normalises wall shear stress of ascending aorta in bicuspid aortic valve. Heart Int. 2020;14(2):121-122. doi:10.17925/HI.2020.14.2.121.
36. Cao K, Atkins SK, McNally A, et al. Simulations of morphotype-dependent hemodynamics in non-dilated bicuspid aortic valve aortas. J Biomech. 2017;50:63–70.
37. McNally A, Madan A, Sucosky P. Morphotype-dependent flow characteristics in bicuspid aortic valve ascending aortas: a benchtop particle image velocimetry study. FrontPhysiol. 2017;8:44.
38. Ando M, Okita Y, Morota T, et al. Thoracic aortic aneurysm associated with congenital bicuspid aorticvalve. Cardiovasc Surg. 1998;6(6):629–634.
39. Piatti F, Sturla F, Bissell MM, et al. 4D flow analysis of BAV-related fluid-dynamic alterations: evidences of wall shear stress alterations in absence of clinically-relevant aortic anatomical remodelling. Front Physiol. 2017;8:441.
40. Michelena HI, Prakash SK, Della Corte A, et al. Bicuspid aortic valve identifying knowledge gaps and rising to the challenge from the international bicuspid aortic valve consortium (BAVCON). Circulation. 2014;129:2691–2704.
41. Riesenkampff E, Fernandes JF, Meier S, et al. Pressure fields by Flow-Sensitive4D, velocity-encoded CMR in patients with aortic coarctation. JACC Cardiovasc Imaging. 2014;7:920–926.
42. Arzani A, Dyverfeldt P, Ebbers T, et al. In vivo validation of numerical prediction for turbulence intensity in an aortic coarctation. Ann Biomed Eng. 2012Apr;40(4):860–870. Epub 2011 Oct 21.
43. LaDisa JF Jr, Alberto Figueroa C, Vignon-Clementel IE, et al. Computational simulations for aortic coarctation: representative results from a sampling of patients. J Biomech Eng. 2011 Sep;133 (9):091008.
44. LaDisa JF Jr, Dholakia RJ, Figueroa CA, et al. Computational simulations demonstrate altered wall shear stress in aortic coarctation patients treated by resection with end-to-end anastomosis. Congenit Heart Dis. 2011 Sep-Oct;65:432–443. Epub. 2011 Jul 31.
45. Capelli C, Sauvage E, Giusti G, et al. Patient specific simulations for planning treatment in congenital heart disease. Interface Focus. 2018;8:20170021.
46. Villafañe J, Feinstein JA, Jenkins KJ, et al. Hot topics in tetralogy of Fallot. J Am Col Cardiol. 2013;62:2155–2166.
47. Paszkowiak JJ, Dardik A. Arterial wall shear stress: observations from the bench to thebedside. Vasc Endovascular Surg. 2003;37:47–57.
48. Fontan F, Baudet E. Surgical repair of tricuspid atresia. Thorax. 1971;26:240–248.
49. Galantowicz M, Cheatham JP, Phillips A, et al. Hybrid approach for hypoplastic left heart syndrome: intermediate results after the learning curve. Ann Thorac Surg. 2008;85:2063–2070.
50. Daley M, d'Udekem Y. The optimal Fontan operation: lateral tunnel or extracardiac conduit? J Thorac Cardiovasc Surg. 2020 Dec 28; S0022-5223(20)33445–0. DOI:10.1016/j.jtcvs.2020.11.179.
51. Migliavacca F, Pennati G, Dubini G, et al. Modeling of the Norwood circulation: effects of shunt size, vascular resistances, and heart rate. Am J Physiol Heart Circ Physiol. 2001;280:H2076–H2086.**••pioneering article of CFD analysis in complex CHDs.**
52. Migliavacca F, Balossino R, Pennati G, et al. Multiscale modelling in biofluidynamics: application to reconstructive paediatric cardiac surgery. J Biomech. 2006;39:1010–1020.
53. Dubini G, de Leval MR, Pietrabissa R, et al. A numerical fluid mechanical study of repaired congenital heart defects. Application to the total cavopulmonary connection. J Biomech. 1996 Jan;29(1):111–121. PMID: 8839024
54. Baker CE, Corsini C, Cosentino D, et al. Modeling of Congenital Hearts Alliance (MOCHA) Investigators. Effects of pulmonary artery banding and retrograde aortic arch obstruction on the hybrid palliation of hypoplastic left heart syndrome. J Thorac Cardiovasc Surg. 2013 Dec;146(6):1341–1348.
55. Corsini C, Migliavacca F, Hsia TY, et al. Modeling of Congenital Hearts Alliance (MOCHA) Investigators. The influence of systemic-to-pulmonary arterial shunts and peripheral vasculature in univentricular circulations: focus on coronary perfusion and aortic arch hemodynamics through computational multi-domain modeling. J Biomech. 2018 Oct 5;79:97–104. Epub. 2018 Aug 4. PMID: 30097266.
56. Rijnberg FM, Hazekamp MG, Wentzel JJ, et al. Energetics of blood flow in cardiovascular disease: concept and clinical implications of adverse energetics in patients with a Fontan circulation. Circulation. 2018;137:2393–2407.
57. Haggerty CM, Restrepo M, Tang E, et al. Fontan hemodynamics from 100 patient-specific cardiac magnetic resonance studies: a computational fluid dynamicsanalysis. Thorac Cardiovasc Surg. 2014;148:1481–1489.
58. Siallagan D, Loke YH, Olivieri L, et al. Virtual surgical planning, flow simulation, and 3-dimensional electrospinning of patient-specific grafts to optimize Fontan hemodynamics. J Thorac Cardiovasc Surg. 2018 Apr;155(4):1734–1742.
59. Trusty PM, Wei ZA, Slesnick TC, et al. The first cohort of prospective Fontan surgical planning patients with follow-up data: how accurate is surgical planning? J Thorac Cardiovasc Surg. 2019 Mar;157 (3):1146–1155.
60. van Bakel TMJ, Lau KD, Hirsch-Romano J, et al. Patient-specific modeling of hemodynamics: supporting surgical planning in a Fontan circulation correction. J Cardiovasc Transl Res. 2018 Apr;11 (2):145–155.
61. Trusty PM, Restrepo M, Kanter KR, et al. A pulsatile hemodynamic evaluation of the commercially available bifurcated Y-graft Fontan modification and comparison with the lateral tunnel and extracardiac conduits. J Thorac Cardiovasc Surg. 2016;151:1529–1536.
62. Cosentino D, Capelli C, Derrick G, et al. Patient-specific computational models to support interventional procedures: a case study of complex aortic re-coarctation. EuroIntervention. 2015;11:669–672.
63. Tang E, Wei ZA, Fogel MA, et al. Fluid-structure interaction simulation of an intra-atrial Fontan connection. Biology (Basel). 2020 Nov 24;9(12):412. PMID: 33255292; PMCID: PMC7760396.
64. Schievano S, Taylor AM, Capelli C, et al., Patient specific finite element analysis results in more accurate prediction of stent fractures: application to percutaneous pulmonary valve implantation. J Biomech. 2010; 43:687–693.10. 1016/j.jbiomech.2009.10.024**••ideal example article of CFD applied to catheter-based interventions.**